Group refractive index quantification using a Fourier domain short coherence Sagnac interferometer

Montonen, Risto

2018-02-15

Montonen , R , Kassamakov , I , Lehmann , P , Österberg , K & Haeggström , E 2018 , ' Group refractive index quantification using a Fourier domain short coherence Sagnac interferometer ' , Optics Letters , vol. 43 , no. 4 , pp. 887-890 . https://doi.org/10.1364/OL.43.000887

http://hdl.handle.net/10138/307965
https://doi.org/10.1364/OL.43.000887

unspecified
acceptedVersion

Group refractive index quantification using Fourier domain short coherence Sagnac interferometer

Risto Montonen,[1,2,*] Ivan Kassamakov,[1,2] Peter Lehmann,[3] Kenneth Österberg,[1,2] and Edward Hæggström[1]

[1]*Department of Physics, University of Helsinki, P.O. Box 64, 00014, Helsinki, Finland*
[2]*Helsinki Institute of Physics, University of Helsinki, P.O. Box 64, 00014, Helsinki, Finland*
[3]*Measurement Technology, Department of Electrical Engineering and Computer Science, University of Kassel, Wilhelmshöher Allee 71, 34121 Kassel, Germany*
**Corresponding author: risto.montonen@helsinki.fi*

Received XX Month XXXX; revised XX Month, XXXX; accepted XX Month XXXX; posted XX Month XXXX (Doc. ID XXXXX); published XX Month XXXX

The group refractive index is important in length calibration of Fourier domain interferometers by transparent transfer standards. We demonstrate accurate group refractive index quantification using a Fourier domain short coherence Sagnac interferometer. Because of a justified linear length calibration function, the calibration constants cancel out in the evaluation of the group refractive index which is then obtained accurately from two uncalibrated lengths. Measurements of two standard thickness coverslips revealed group indices of 1.5426 ± 0.0042 and 1.5434 ± 0.0046, with accuracies quoted at 95% confidence level. This agreed with the dispersion data of coverslip manufacturer and therefore validates our method. Our method provides a sample specific and accurate group refractive index quantification using the same Fourier domain interferometer that is to be calibrated for the length. This reduces significantly the requirements of the calibration transfer standard.

OCIS codes: (120.3180) Interferometry; (120.3940) Metrology.

http://dx.doi.org/10.1364/OL.99.099999

Length calibration of point-by-point detection Fourier domain interference profilometers by step structures requires a translation stage to obtain a step profile. The translation, unfortunately, induces extra uncertainty sources that inflate the final measurement uncertainty. Length calibration through transparent specimens, e.g. glass plates, overcomes this problem. However, the absolute (not relative to air) group refractive index, n_g, of the specimen needs to be known to convert the specified geometric thickness into optical thickness [1]. Several methods to measure the refractive index of solids exist. Refractometers based on measuring the critical angle or the angle of refraction are limited by the sample size and shape, and require a predefined scale to read the index value [2,3]. Polarimetric and surface plasmon resonance methods are sensitive but employ cumbersome models to extract the dielectric function of the sample [4,5]. Interference microscope methods can quantify n_g [6-8]. However, their accuracy relies on calibrated interference and confocal scanners and on the objectives' working numerical aperture. In a paper by Yao *et al.* [8] these sources of uncertainty have thoroughly been accounted for when calculating the refractive index uncertainty. In contrast, Fourier domain Mach-Zehnder interferometer [9] measures n_g without moving parts. To have accurate results the two light beams of the Mach-Zehnder interferometer need to be balanced, i.e., the optical path lengths of the interfering light beams are set equal, which is difficult because the two light beams share no optical components.

The phase refractive index, n_p, of a medium is defined as the ratio between the phase velocity of light in vacuum and in the medium, which is a dimensionless quantity. In interferometry the refractive index is typically evaluated as h/H, where h is the optical thickness and H is the geometric thickness. The quantities n_g and n_p are related to each other through the expression

$$n_g = n_p - \lambda \frac{dn_p}{d\lambda}, \tag{1}$$

where λ is the wavelength of light in vacuum. The group index defining the propagation velocity of a wave packet in a medium is important in interferometry: As the spatial location of the energy maximum defines the length measured by an interferometer, the index related to the measured length is the group index [10].

In this letter we present accurate n_g quantification for transparent samples using a Fourier domain short coherence Sagnac interferometer. We give insight into the n_g evaluation by showing that in the Fourier domain short coherence Sagnac interferometer an accurate n_g is quantified from two uncalibrated lengths. Finally, n_g quantified for two glass coverslips are compared against the manufacturer's data to test the validity of our method.

Figure 1 depicts the setup. Light from a light emitting diode (LED: Kingbright, L-793SRC-E, 30 mA forward current, central wavelength λ_0 = 658 nm, –3 dB bandwidth 21 nm) was coupled into a multimode fiber (MMF: Newport, F-MSD-C-1FC) using lens 1 and an objective (L1: Thorlabs, ACL2520-B; and O: Olympus, Plan N 10x/0.25). The fiber-coupled light was collimated by lens 2 (L2: Thorlabs, ACL2520-B) and stopped by an iris to ca. 1 mm beam diameter. This collimated input light beam was directed into a Sagnac interferometer through a cube beam splitter (BS1: Thorlabs, BS016, $\lambda/10$ flatness at 633 nm, side length 20 mm). The Sagnac interferometer (Fig. 1, dashed box) was formed by a second cube beam splitter (BS2: Optosigma, 039-0265, $\lambda/4$ flatness at 633 nm, side length 20 mm) and two silver mirrors (M1: Edmund Optics, #43-412-577, $\lambda/20$ flatness at 633 nm, 25.4 mm diameter; and M2: Edmund Optics, #32-195-577, $\lambda/10$ flatness at 633 nm, 25.4 mm diameter). In this configuration the BS2 splits the light into clockwise and counterclockwise light beams which are then steered back into BS2 by M1 and M2. The recombined Sagnac output beam was focused by lens 3 (L3: Thorlabs, LA1805-B) into a fiber-optic spectrometer (Ocean Optics, HR2000+) which recorded the spectral interference data. Applying spectral data acquisition (spectral resolution, $\delta\lambda$, ~0.44 nm) no reference mirror scanner was needed. The two light beams in the Sagnac interferometer were balanced to zero optical path length difference with use of interference: Close to complete beam recombination, interference modulation was achieved, and the zero difference was found by adjusting the mirrors in an effort to maximize the recorded intensity. Compared to the Sagnac interferometer used here, the Mach-Zehnder configuration would require much more effort to ensure zero optical path length difference of the two interferometer arms. The two beams were balanced in a displaced configuration. This is beneficial since if the sample partly cuts both beams the measurement result is biased in a way that depends on the beam footprints and on the beam orientations. We avoided this bias by placing the sample to cut only one of the beams. The chosen interferometer configuration limits the measurement area as only positions near the sample edge (3 mm) can be measured.

Coverslips of standard thicknesses #00 and #0, having nominal thicknesses of 70 µm and 100 µm respectively, were used as samples. These samples were chosen since coverslips are stable and flat which makes them ideal as a calibration transfer standard and since they have a suitable thickness considering the maximum optical measurement range of our device, $\lambda_0^2/(4\delta\lambda)$ = 240 µm. The coverslips were placed into the clockwise beam path in a slightly slanted orientation, < 2°, (0.2° acceptance angle) to capture sample reflections with the same fiber-optic spectrometer, Fig. 1. The coverslips were oriented by maximizing the intensity of the recorded reflections.

The sample modifies the clockwise beam path and generates two distinctive interference peaks in the A-scan, see Fig. 2. A-scans, used in optical coherence tomography, are typically shown with a horizontal axis that is half of the optical path length. This is to indicate optical thickness correctly in reflection mode measurements where the light undergoes a path length that is twice the optical thickness. In this way peak h (Fig. 2, right inset) measures, under a small angle approximation, the optical thickness, h, of the sample. Peak A accounts for the optical path length difference between the modified beam path and the

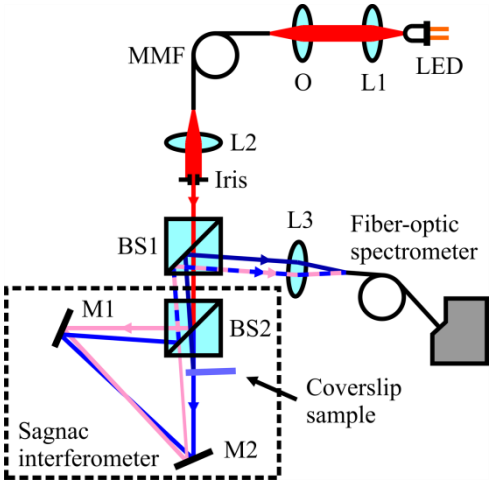

Fig. 1. Fourier domain short coherence Sagnac interferometer setup to determine the group refractive index. Dashed box highlights the Sagnac interferometer configuration. LED, light emitting diode; L, lens; O, objective; MMF, multimode fiber; BS, beam splitter; M, mirror; —, input light beam; —, clockwise light beam; —, counterclockwise light beam; —, Sagnac output light beam; —, sample reflections.

unmodified counterclockwise beam path. Because the measured lengths in the A-scans are half of the corresponding optical path lengths, the optical path length difference equals the measured A multiplied by 2. This difference describes the added optical path length in the modified beam path where the path through the sample of geometric thickness H and group refractive index $n_{g,\,sample}$ replaces a corresponding path in air. Under the small angle approximation we get

$$2A \approx n_{g,\,sample} H - n_{g,\,air} H = h - n_{g,\,air} H. \quad \textbf{(2)}$$

From Eq. (2) the geometric thickness of the sample is

$$H \approx \frac{h - 2A}{n_{g,\,air}}, \quad \textbf{(3)}$$

whereas the group refractive index of the sample is

$$n_{g,\,sample} = \frac{h}{H} \approx \frac{h}{h - 2A} n_{g,\,air}. \quad \textbf{(4)}$$

A-scans revealing the peaks h and A were extracted from 100 recorded spectral interferograms (Fig. 2, left inset, light intensity at wavenumber bins). The spectral interferograms were first resampled to equispaced wavenumber space by implementing a treatment described by Gora *et al.* [11] on an interference signal from a 50 µm thick air gap. Air causes negligible dispersion and, therefore, it was considered appropriate. The resampled data were then inverse fast Fourier transformed. The nominal 50 µm air gap thickness was used to scale the horizontal axis of the A-scans. In the Sagnac interferometer (Fig. 1, dashed box), the dispersion of the optical components was effectively matched because the two counter propagating light beams were balanced and they shared the same optical components. The measured lengths, h_M and A_M, were determined as average peak positions, N = 100.

The n_g of air at λ_0 = 658 nm, in stable measurement conditions of temperature (22.9 ± 0.6) °C, atmospheric pressure (100807 ± 16) Pa, and relative humidity (36.3 ± 2.0)%, was approximated

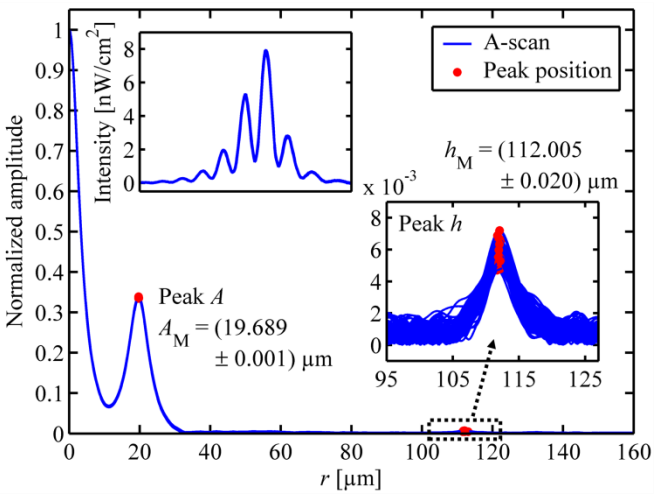

Fig. 2. Fourier domain short coherence Sagnac interferometer A-scan revealing the optical thickness of the #00 coverslip sample, peak h, and the Sagnac beam path difference, peak A. h_M and A_M represent the measured lengths. A-scan amplitude normalized to the DC peak at zero optical length, r. Insets: Peak h close-up view (right inset); spectral interferogram, light intensity at wavenumber bins, 100 repeats (left inset).

using the Edlén equation [12,13]. This gave $n_{g,\,air} - 1 = (274.3 \pm 0.6) \times 10^{-6}$, where all uncertainties represent standard uncertainty. The temperature and relative humidity were recorded using a data logger (Clas Ohlson, 36-4208-1/ST-171), whereas the atmospheric pressure was recorded using a pressure sensor (Vaisala, PTB100A).

No length calibration is required to estimate accurate $n_{g,\,sample}$. The dilation property of the Fourier transform [14] ensures that any error in bin width in the equispaced wavenumber space dilates the length space linearly. Thus the calibration function, C, of any Fourier domain interferometer is linear with respect to the optical length, r; that is, $C = ar$, where a is the calibration constant [1]. The calibrated optical length is $r_C = r - C$ [15]. Taking this into account, the calibrated lengths h_C and A_C become $h_M(1 - a)$ and $A_M(1 - a)$. Evaluating $n_{g,\,sample}$, Eq. (4), by using the calibrated lengths h_C and A_C, the calibration constant cancels out and an accurate $n_{g,\,sample}$ result is evaluated directly from h_M and A_M. In the literature optical self-calibration measurement methods have been presented. These are based on second-harmonic generation [16] and on a heterodyne Mach-Zehnder interferometer [17].

The measurement gave $n_{g,\,sample} = 1.5426 \pm 0.0042$ for the #00 coverslip and 1.5434 ± 0.0046 for the #0 coverslip at $\lambda_0 = 658$ nm. For a completely balanced setup one measurement took less than two minutes. The uncertainties are quoted at 95% confidence level and combine contributions from random uncertainties in sample orientation, h_M, and A_M, and from systematic uncertainties arising from $n_{g,\,air}$ and balancing that were common for the two samples. The uncertainties were evaluated using the Guide to the expression of uncertainty in measurement [18]. Table 1 summarizes the uncertainty budget for the #00 coverslip sample. The sample orientation is related in a complicated way to the cosine and wavefront errors in the system. The wavefront error affects the phase at the receiver and it includes both the imaging aberrations and the aberration caused by the sample flatness. We estimated the uncertainty contribution of the sample orientation by measuring $n_{g,\,sample}$ across the system's acceptance angle. From this the uncertainty contribution was evaluated by the minimum-maximum method. The slanted sample orientation causes a biasing cosine error, see Fig. 3. Taking this into account, $n_{g,\,sample}$ becomes

$$\frac{b}{b-2A}\cos(\theta_1-\theta_2)n_{g,\,air},$$

where b is the cosine erroneous optical thickness of the sample, θ_1 is the angle of incidence, and θ_2 is the angle of refraction. In a slanted sample (2°) this causes a bias on the order of 10^{-4} and thus the biasing cosine error was neglected in our analysis. Standard uncertainties for h_M and A_M, and the correlation between h_M and A_M were obtained from the repeated A-scans. Finally, since variation in the Sagnac interferometer balancing causes zero centered variation into the balanced optical path length difference, we estimated the systematic balancing uncertainty by measuring the variation in A when the balancing was repeated 10 times.

Table 1. Group refractive index uncertainty budget for #00 coverslip sample. The total uncertainty obtained as the root sum of squares from the random and systematic uncertainty components.

Group refractive index, $n_{g,\,sample}$			**1.5426**
Uncertainty component		Contribution, $u_i(y)$	
		Rand.	Sys.
Measured optical thickness	h_M	1.5×10^{-4}	
Sagnac beam path difference	A_M	3.9×10^{-5}	
Sample orientation		2.1×10^{-3}	
Group refractive index of air	$n_{g,\,air}$		8.1×10^{-7}
Balancing			3.8×10^{-4}
Correlated uncertainty component		Contribution, $u_k(y)$ (in squared units)	
Correlation between h_M and A_M		1.6×10^{-9}	
Standard uncertainty, $u_c(y) = \left(\sum_i u_i^2(y) + \sum_k u_k(y)\right)^{1/2}$		Rand.	2.1×10^{-3}
		Sys.	3.8×10^{-4}
Total at 95% confidence level, $U = 2u_c(y)$			**4.2×10^{-3}**

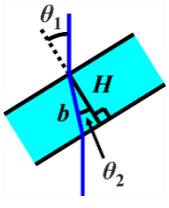

Fig. 3. Cosine error geometry associated with a slanted sample. H, the geometric thickness of the sample; b, the cosine erroneous optical thickness of the sample; θ_1, the angle of incidence; and θ_2, the angle of refraction.

The n_g measurement of #00 and #0 standard thickness coverslips shows overlapping results as expected since both samples were produced from the same glass material. In addition, using Eq. (1) the manufacturer's dispersion data converted into an absolute index gives n_g = 1.5445 at λ_0 = 658 nm. This value is within the measurement uncertainty and verifies the validity of the presented method.

The quantified n_g are reported at the central wavelength of the light source, λ_0. However, since the method is based on the coherence of light, we note, that a more accurate theory needs to account for the central wavelength of the interference signal rather than for λ_0 [19]. The interference wavelength is affected by spatial coherence effects such as scattering that on random rough surfaces attenuates the coherence more at shorter wavelengths than at longer wavelengths. The central wavelength shift caused by this phenomenon increases with the light source's bandwidth. For a narrow band LED the shift is at maximum 1 nm.

The group refractive index expression, Eq. (1), neglects higher order dispersion. However, the group velocity dispersion has only a minor effect on the quantified n_g because of the narrow band LED and small sample thickness. Thus the quantified n_g could be considered consistent with the result derived using Eq. (1). Considering Eq. (1) further, the phase index cannot be solved unambiguously from the group index data. Fortunately, an empirical study by Rogers and Hopler [20] suggests that for standard glasses the phase index could be converted from the group index data, measured at least at three wavelengths, with an accuracy of 0.0016.

We use the sample specific and accurate group refractive index data to convert the specified geometric thickness of a calibration transfer standard into optical thickness. Thus no prior knowledge of refractive index or cumbersome measurements are required on the transfer standard. The measured optical thickness of the transfer standard further completes the data matrix required for the length calibration. Finally, this gives us the calibration function of the device [1].

We demonstrated accurate group refractive index quantification of transparent samples with a Fourier domain short coherence Sagnac interferometer. Since Fourier domain interferometers have a linear length calibration function we could evaluate the group refractive index accurately from two uncalibrated lengths. A comparison of the results for two glass coverslips against the manufacturer's dispersion data verified the validity of the presented method. Considering the calibration of Fourier domain interferometers, we expect that our method improves the feasibility of using glass plates as a calibration transfer standard since a sample specific and accurate n_g could be quantified using the same device that is to be calibrated for the length.

Funding. Academy of Finland (127847); Deutscher Akademischer Austauschdienst (DAAD) (57071091); European Laboratory for Particle Physics (CERN) (KE-2488).

References

1. R. Montonen, I. Kassamakov, E. Hæggström, and K. Österberg, Appl. Opt. **54**, 4635 (2015).
2. P. Herrmann, Appl. Opt. **19**, 3261 (1980).
3. I. D. Nikolov, and C. D. Ivanov, Appl. Opt. **39**, 2067 (2000).
4. E. Garcia-Caurel, A. De Martino, J.-P. Gaston, and L. Yan, Appl. Spectrosc. **67**, 1 (2013).
5. K. Peterlinz, and R. Georgiadis, Opt. Commun. **130**, 260 (1996).
6. N. Sandler, I. Kassamakov, H. Ehlers, N. Genina, T. Ylitalo, and E. Haeggstrom, Sci. Rep. **4**, 4020 (2014).
7. M. Haruna, M. Ohmi, T. Mitsuyama, H. Tajiri, H. Maruyama, and M. Hashimoto, Opt. Lett. **23**, 966 (1998).
8. J. Yao, J. Huang, P. Meemon, M. Ponting, and J. P. Rolland, Opt. Express **23**, 30149 (2015).
9. J. Park, J. Bae, J. Jin, J.-A. Kim, and J. W. Kim, Opt. Express **23**, 32941 (2015).
10. A. Bers, Am. J. Phys. **68**, 482 (2000).
11. M. Gora, K. Karnowski, M. Szkulmowski, B. J. Kaluzny, R. Huber, A. Kowalczyk, and M. Wojtkowski, Opt. Express **17**, 14880 (2009).
12. K. Birch, and M. Downs, Metrologia **31**, 315 (1994).
13. A. L. Buck, J. Appl. Meteorol. **20**, 1527 (1981).
14. D. W. Kammler, *A first course in Fourier analysis* (Cambridge University Press, 2007).
15. R. Montonen, I. Kassamakov, E. Hæggström, and K. Österberg, Opt. Eng. **55**, 014103 (2016).
16. H. Li, G. B. Rieker, X. Liu, J. B. Jeffries, and R. K. Hanson, Appl. Opt. **45**, 1052 (2006).
17. S. Zhang, H. Wang, X. Zou, Y. Zhang, R. Lu, and Y. Liu, Opt. Lett. **39**, 3504 (2014).
18. BIPM, IEC, IFCC, ILAC, ISO, IUPAC, IUPAP, and OIML, *Evaluation of measurement data – Guide to the expression of uncertainty in measurement* (JCGM, 2008).
19. R. Montonen, A. Nolvi, S. Tereschenko, P. Kühnhold, P. Lehmann, E. Hæggström, and I. Kassamakov, Opt. Express **25**, 12090 (2017).
20. J. R. Rogers, and M. D. Hopler, J. Opt. Soc. Am. A **5**, 1595 (1988).

References

1. R. Montonen, I. Kassamakov, E. Hæggström, and K. Österberg, "Calibration of Fourier domain short coherence interferometer for absolute distance measurements," Applied Optics **54**, 4635–4639 (2015).
2. P. Herrmann, "Determination of thickness, refractive index, and dispersion of waveguiding thin films with an Abbe refractometer," Applied Optics **19**, 3261–3262 (1980).
3. I. D. Nikolov and C. D. Ivanov, "Optical plastic refractive measurements in the visible and the near-infrared regions," Applied Optics **39**, 2067–2070 (2000).
4. E. Garcia-Caurel, A. De Martino, J.-P. Gaston, and L. Yan, "Application of spectroscopic ellipsometry and Mueller ellipsometry to optical characterization," Applied Spectroscopy **67**, 1–21 (2013).
5. K. Peterlinz and R. Georgiadis, "Two-color approach for determination of thickness and dielectric constant of thin films using surface plasmon resonance spectroscopy," Optics Communications **130**, 260–266 (1996).
6. N. Sandler, I. Kassamakov, H. Ehlers, N. Genina, T. Ylitalo, and E. Haeggstrom, "Rapid interferometric imaging of printed drug laden multilayer structures," Scientific Reports **4**, 4020 (2014).
7. M. Haruna, M. Ohmi, T. Mitsuyama, H. Tajiri, H. Maruyama, and M. Hashimoto, "Simultaneous measurement of the phase and group indices and the thickness of transparent plates by low-coherence interferometry," Optics Letters **23**, 966–968 (1998).
8. J. Yao, J. Huang, P. Meemon, M. Ponting, and J. P. Rolland, "Simultaneous estimation of thickness and refractive index of layered gradient refractive index optics using a hybrid confocal-scan swept-source optical coherence tomography system," Optics Express **23**, 30149–30164 (2015).
9. J. Park, J. Bae, J. Jin, J.-A. Kim, and J. W. Kim, "Vibration-insensitive measurements of the thickness profile of large glass panels," Optics Express **23**, 32941–32949 (2015).
10. A. Bers, "Note on group velocity and energy propagation," American Journal of Physics **68**, 482–484 (2000).
11. M. Gora, K. Karnowski, M. Szkulmowski, B. J. Kaluzny, R. Huber, A. Kowalczyk, and M. Wojtkowski, "Ultra high-speed swept source OCT imaging of the anterior segment of human eye at 200 kHz with adjustable imaging range," Optics Express **17**, 14880–14894 (2009).
12. K. Birch and M. Downs, "Correction to the updated Edlén equation for the refractive index of air," Metrologia **31**, 315–316 (1994).
13. A. L. Buck, "New equations for computing vapor pressure and enhancement factor," Journal of Applied Meteorology **20**, 1527–1532 (1981).
14. D. W. Kammler, *A first course in Fourier analysis*, Cambridge University Press (2007), pp. 138–140.
15. R. Montonen, I. Kassamakov, E. Hæggström, and K. Österberg, "Quantifying height of ultraprecisely machined steps on oxygen-free electronic copper disc using Fourier-domain short coherence interferometry," Optical Engineering **55**, 014103 (2016).
16. H. Li, G. B. Rieker, X. Liu, J. B. Jeffries, and R. K. Hanson, "Extension of wavelength-modulation spectroscopy to large modulation depth for diode laser absorption measurements in high-pressure gases," Applied Optics **45**, 1052–1061 (2006).
17. S. Zhang, H. Wang, X. Zou, Y. Zhang, R. Lu, and Y. Liu, "Self-calibrating measurement of high-speed electro-optic phase modulators based on two-tone modulation," Optics Letters **39**, 3504–3507 (2014).
18. BIPM, IEC, IFCC, ILAC, ISO, IUPAC, IUPAP, and OIML, *Evaluation of measurement data – Guide to the expression of uncertainty in measurement*, JCGM (2008).
19. R. Montonen, A. Nolvi, S. Tereschenko, P. Kühnhold, P. Lehmann, E. Hæggström, and I. Kassamakov, "System spectrum conversion from white light interferogram," Optics Express **25**, 12090–12099 (2017).
20. J. R. Rogers and M. D. Hopler, "Conversion of group refractive index to phase refractive index," Journal of the Optical Society of America A **5**, 1595–1600 (1988).